

MicroRNA-30c Mimic Mitigates Hypercholesterolemia and Atherosclerosis in Mice^{*[5]}

Received for publication, March 21, 2016, and in revised form, May 28, 2016. Published, JBC Papers in Press, June 30, 2016, DOI 10.1074/jbc.M116.728451

Sara Irani^{†§}, Xiaoyue Pan[§], Bailey C. E. Peck^{||}, Jahangir Iqbal[§], Praveen Sethupathy^{||}, and M. Mahmood Hussain^{§***††}

From the [†]Molecular and Cell Biology Program, School of Graduate Studies and [§]Departments of Cell Biology and Pediatrics, State University of New York (SUNY) Downstate Medical Center, Brooklyn, New York 11203, ^{||}Curriculum in Genetics and Molecular Biology, ^{||}Department of Genetics, University of North Carolina, Chapel Hill, North Carolina 27599, ^{**}Veterans Affairs New York Harbor Healthcare System, Brooklyn, New York 11422, and ^{††}Winthrop University Hospital, Mineola, New York 11501

High plasma cholesterol levels are a major risk factor for atherosclerosis. Plasma cholesterol can be reduced by inhibiting lipoprotein production; however, this is associated with steatosis. Previously we showed that lentivirally mediated hepatic expression of microRNA-30c (miR-30c) reduced hyperlipidemia and atherosclerosis in mice without causing hepatosteatosis. Because viral therapy would be formidable, we examined whether a miR-30c mimic can be used to mitigate hyperlipidemia and atherosclerosis without inducing steatosis. Delivery of a miR-30c mimic to the liver diminished diet-induced hypercholesterolemia in C57BL/6J mice. Reductions in plasma cholesterol levels were significantly correlated with increases in hepatic miR-30c levels. Long term dose escalation studies showed that miR-30c mimic caused sustained reductions in plasma cholesterol with no obvious side effects. Furthermore, miR-30c mimic significantly reduced hypercholesterolemia and atherosclerosis in *ApoE*^{-/-} mice. Mechanistic studies showed that miR-30c mimic had no effect on LDL clearance but reduced lipoprotein production by down-regulating microsomal triglyceride transfer protein expression. MiR-30c had no effect on fatty acid oxidation but reduced lipid synthesis. Additionally, whole transcriptome analysis revealed that miR-30c mimic significantly down-regulated hepatic lipid synthesis pathways. Therefore, miR-30c lowers plasma cholesterol and mitigates atherosclerosis by reducing microsomal triglyceride transfer protein expression and lipoprotein production and avoids steatosis by diminishing lipid syntheses. It mitigates atherosclerosis most likely by reducing lipoprotein production and plasma cholesterol. These findings establish that increasing hepatic miR-30c levels is a viable treatment option for reducing hypercholesterolemia and atherosclerosis.

Atherosclerosis, hardening of the arteries secondary to lipid deposition, is the major cause of morbidity and mortality in the United States (1–3). High plasma cholesterol levels are a major risk factor for cardiovascular diseases, and their reduction is a national goal (2, 4). Currently, statins are the standard of care. They lower plasma cholesterol by reducing cholesterol synthesis and enhancing the rate of removal of lipoproteins from the plasma. Statins lower plasma cholesterol by 20–30% and cardiovascular disease mortality by 30–40% (5–8). Recently, proprotein convertase subtilisin/kexin type 9 (PCSK9)² inhibitors have emerged as potential new drugs for the treatment of hyperlipidemia (9). PCSK9 binds to LDL receptor and targets it for lysosomal degradation. Thus, inhibition of PCSK9 leads to increased LDL receptor expression, increased clearance of lipoproteins, and decreased plasma LDL cholesterol levels (10–12). Because both statins and PCSK9 antibodies reduce plasma cholesterol by modulating LDL receptor expression, they are ineffective in homozygous familial hypercholesterolemia subjects with <2% of the LDL receptor activity (11, 13, 14). In addition, a significant percentage of the general population experiences significant side effects with statins and PCSK9 inhibitors (13–15).

A complementary approach to lower plasma cholesterol is to inhibit lipoprotein synthesis and secretion to reduce their entry into the circulation. Lipoprotein production requires a structural protein apolipoprotein B (apoB) and a chaperone, microsomal triglyceride transfer protein (MTP) (16, 17). Because apoB does not have any measurable activity, its levels have been lowered using an antisense oligonucleotide, mipomersen (8, 18). This drug has been approved for the treatment of familial hypercholesterolemia subjects who have high plasma cholesterol and do not respond to statins (19). However, compared with apoB, MTP has been a more favored target to lower plasma lipids because its lipid transfer activity can be measured *in vitro* and it is amenable to high throughput screening for drug development. Virtually all of the major pharmaceutical companies have, at some point, developed drugs that potently inhibit MTP activity and lower plasma lipids. However, these drugs increase plasma transaminases, markers of liver injury, fatty liver dis-

* This work was supported in part by National Institutes of Health Genetics and Molecular Biology Training Grant T32GM-709239 (to B. C. E. P.); National Institutes of Health Grant DK-091318 (to P. S.); an American Heart Association predoctoral fellowship (to S. I.); and National Institutes of Health Grants DK-46900 and DK-081879, Veterans Affairs Merit Award BX001728, and a technology accelerator fund grant from SUNY Research Foundation (to M. M. H.). The authors declare that they have no conflicts of interest with the contents of this article. The content is solely the responsibility of the authors and does not necessarily represent the official views of the National Institutes of Health.

[5] This article contains supplemental Table S1.

[†] To whom correspondence should be addressed: Dept. of Cell Biology, SUNY Downstate Medical Center, 450 Clarkson Ave., Brooklyn, NY 11203. Tel.: 718-270-4790; Fax: 718-270-2462; E-mail: Mahmood.Hussain@downstate.edu.

² The abbreviations used are: PCSK9, proprotein convertase subtilisin/kexin type 9; apo, apolipoprotein; ALT, alanine aminotransferase; AST, aspartate aminotransferase; CK, creatine kinase; miR, microRNA; MTP, microsomal triglyceride transfer protein; Scr, scrambled control miR; RISC, RNA-induced silencing complex; RNA-seq, RNA sequencing; FDR, false discovery rate.

MiR-30c Mimic and Hyperlipidemia

ease, and hepatosteatosis (20–23). One MTP inhibitor, lomitapide, has been approved for the treatment of familial hypercholesterolemia (8, 24, 25). Both lomitapide and mipomersen carry warning labels for hepatic steatosis. Hence, there is a need for new drugs that can lower plasma lipids while avoiding steatosis.

Discovery of endogenous microRNAs (miRs) provides a new way of treating dyslipidemia and associated cardiovascular disease (26, 27). MiRs are endogenous gene products of ~22 nucleotides. They interact predominantly with the 3'-untranslated regions (3'-UTRs) of target mRNAs and reduce protein synthesis by augmenting mRNA degradation or by diminishing translation (28, 29); mRNA degradation appears to be the major mechanism in mammalian systems (30). Different miRs and anti-miRs are in clinical trials for the treatment of various pathologies (31–33) and are expected to be the drugs of the future.

Our previous work showed that lentivirally mediated overexpression of miR-30c decreases hepatic MTP expression and activity, lowers plasma cholesterol, and reduces hepatic lipoprotein production without altering hepatic lipids and plasma transaminases in Western diet-fed C57BL/6J (WT) mice (34). Also, lentivirally mediated hepatic overexpression of miR-30c reduced plasma cholesterol and mitigated atherosclerotic plaques in Western diet-fed *ApoE*^{-/-} mice (34). Because viral delivery to humans for therapeutic use may pose several challenges, we hypothesize that miR-30c analogues can be used to treat hypercholesterolemia and atherosclerosis in statin-intolerant and familial hypercholesterolemia patients. To begin testing this hypothesis, we performed preclinical studies using a stabilized analogue of miR-30c ("mimic") to evaluate its efficacy and molecular mechanisms in lowering plasma cholesterol and atherosclerosis in mice.

Results

Custom Synthesized MiR-30c Mimic Reduces MTP Expression and ApoB Secretion in Human Hepatoma Cells

To test the biological potency of the custom synthesized mimic, we transfected human hepatoma Huh-7 cells with the miR-30c mimic or a scrambled control miR (Scr) (Fig. 1). Increasing concentrations of miR-30c mimic significantly reduced MTP activity and apoB secretion compared with Scr (Fig. 1, *a* and *b*). The effect of miR-30c reached a maximum at 50 nM. This mostly likely represents saturation of RISC machinery with miR-30c-RISC complexes. Furthermore, time course studies revealed that maximum reductions in MTP activity and apoB secretion occurred 48 h after transfections, and the effect of miR-30c was lost after 96 h (Fig. 1, *c* and *d*). These results are in concert with our previous studies (34), suggesting that the custom synthesized miR-30c mimic is biologically active in reducing MTP activity and apoB secretion in hepatoma cells.

MiR-30c Mimic Mitigates Progression of Diet-induced Hypercholesterolemia in Mice

To determine whether the mimic can prevent progression of diet-induced hyperlipidemia, miR-30c mimic and Scr were complexed with lipid emulsions and injected into male WT mice placed on a Western diet (Fig. 2). Plasma cholesterol

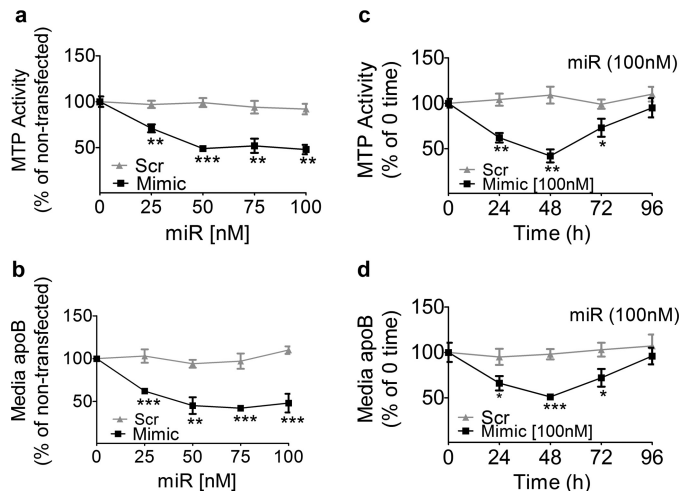


FIGURE 1. Effect of different concentrations of miR-30c mimic on cellular MTP activity and apoB secretion in Huh-7 cells. *a* and *b*, MTP activity (percent triglyceride transfer $\text{mg}^{-1} \text{h}^{-1}$) in cells (*a*) and apoB concentrations (ng mg^{-1} of cell protein; determined by ELISA) (*b*) in culture media of Huh-7 cells transfected with increasing concentrations of Scr or miR-30c mimic measured 48 h after transfection. MTP activity and apoB secretion were normalized to non-transfected cells. There was no significant difference between non-transfected and Scr-transfected cells (not shown). *c* and *d*, time course of changes in MTP activity (*c*) and apoB concentration (*d*) in cells and media, respectively, transfected with 100 nM Scr or miR-30c mimic. MTP activity and apoB secretion at time 0 were set to 100%. The data are representative of two independent experiments. All data are shown as the mean \pm S.D. *, $p < 0.05$; **, $p < 0.01$; ***, $p < 0.001$. Standard deviations are presented as error bars.

increased in both miR-30c mimic- and Scr-injected groups. However, increases in plasma cholesterol levels were significantly lower (–21 to 26%) in the miR-30c mimic group compared with the Scr group (Fig. 2*a*). Fasting plasma triglyceride, alanine aminotransferase (ALT), aspartate aminotransferase (AST), glucose (Fig. 2, *b–e*), and creatine kinase (CK) levels were not different between the two groups. Moreover, we did not see changes in food intake between both groups. Analyses of different tissues showed that miR-30c levels increased by 6- and 15-fold in the livers and spleens, respectively, of mice receiving the mimic; there were no significant differences in miR-30c levels in the kidney, heart, and jejunum (Fig. 2*f*). In a separate experiment, we observed that miR-30c was not delivered to adipose tissue (data not shown). In contrast to miR-30c, the hepatic levels of another miR-30 family member, miR-30b, were unaffected (Fig. 2*g*). Hepatic MTP activity was significantly reduced (–42%) in the miR-30c mimic group (Fig. 2*h*) with no effect on hepatic triglyceride and cholesterol levels (Fig. 2, *i* and *j*). These studies suggest that the delivery of miR-30c mimic to the liver curtailed progression of diet-induced hypercholesterolemia with no effect on hepatic lipids and plasma enzymes.

Regression of Diet-induced Hypercholesterolemia by MiR-30c Mimic

Next, we asked whether miR-30c mimic can reduce plasma cholesterol in hyperlipidemic mice. Male WT mice were fed a Western diet for 4 weeks to induce hyperlipidemia and divided into three groups. One group received PBS, and the other two groups received different doses of either miR-30c mimic or Scr. There were no significant differences between PBS and Scr

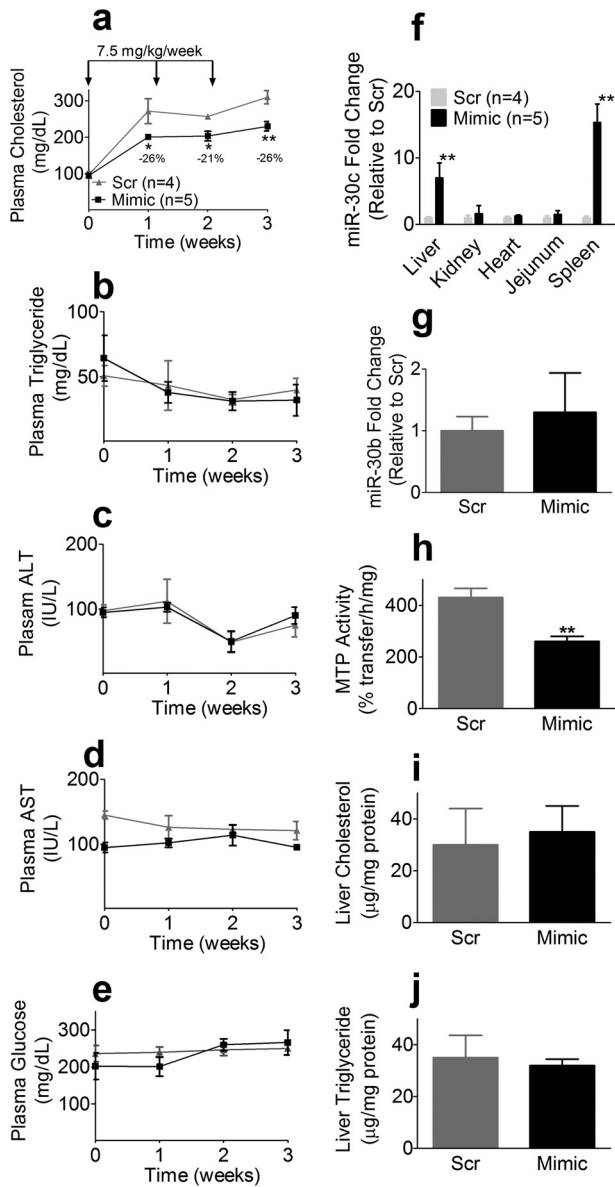


FIGURE 2. MiR-30c mimic dampens progression of diet-induced hypercholesterolemia. Male C57BL/6J mice (8 weeks old) were injected with 7.5 mg/kg/week miR-30c mimic ($n = 5$) or Scr miR ($n = 4$) complexed with lipid emulsions and started on a Western diet. Fasting plasma was collected on day 6 after each injection to measure cholesterol (a), triglyceride (b), ALT (c), AST (d), and glucose (e). 48 h after the last injection, mice were euthanized. Different tissues were also collected to measure miR-30c levels (f). Hepatic tissues were used to measure miR-30b (g), MTP activity (h), cholesterol (i), and triglyceride (j). * $p < 0.05$; ** $p < 0.01$; *** $p < 0.001$ as determined by Student's t test. Standard deviations are presented as error bars.

groups for the various metabolic parameters studied (Fig. 3), indicating that Scr does not affect these parameters. MiR-30c mimic did not affect plasma cholesterol at a single dose of 2.5 mg/kg/week compared with Scr and PBS groups. However, at a 5 mg/kg/week dose, significant sustained reductions in plasma cholesterol levels were seen in the mimic group compared with the Scr or PBS group, reaching a maximal reduction of 38% (Fig. 3a). Plasma triglyceride, AST, and ALT in the mimic group were not significantly different from those in the Scr and PBS groups (not shown). These studies indicate that miR-30c mimic reduces plasma cholesterol in Western diet-fed hyperlipidemic mice without affecting plasma triglyceride and transaminases.

Tissue analysis revealed that miR-30c levels increased by 13- and 20-fold in the livers and spleens, respectively, but remained unchanged in kidney, heart, and jejunum of mice injected with the mimic (Fig. 3b). Contrary to miR-30c, hepatic miR-30b was not increased in the mimic-injected group compared with control groups (Fig. 3c). Expression levels of miR-30c putative target genes (*Mtpp*, *Lpgat1*, *Qki*, and *Elovl5*) were significantly reduced in the mimic group compared with the PBS and Scr groups, whereas no significant changes were observed for non-target genes (*ApoA1* and *Gapdh*) (Fig. 3d). Additionally, MTP activity was significantly lower in the mimic group compared with control groups (Fig. 3e). Moreover, there were no significant differences in hepatic cholesterol and triglyceride levels (not shown). These studies show that miR-30c reduced hepatic MTP activity without causing steatosis.

The studies in Figs. 2 and 3 showed that miR-30c injections reduced plasma cholesterol and increased hepatic miR-30c levels. To determine whether these two observations were related, we carried out a Spearman correlation analysis. There was a significant positive correlation between increases in hepatic miR-30c levels and percent reductions in plasma cholesterol levels. The slope of the curve was ~ 2 , predicting that a ~ 2 -fold increase in hepatic miR-30c might reduce plasma cholesterol by 50%. Thus, there is a significant positive correlation between hepatic miR-30c accretions and plasma cholesterol reduction.

Time Course and Long Term Dose Escalation Studies Revealed Sustained Reductions in Plasma Cholesterol

Next, we studied the time course and long term effects of escalating doses of miR-30c mimic in female WT mice that were fed a Western diet for 4 weeks (Fig. 4). In previous studies, we used male mice. Here, we used females to demonstrate universality of miR-30c effects. After a single injection of 5 mg/kg/week miR-30c mimic, significant reductions in plasma cholesterol were evident on day 2, and the highest reduction of 21% was on day 6 (Fig. 4a). After day 10, plasma cholesterol reverted to normal levels as in the PBS group. Next, we asked whether successive injections would elicit a similar response. Two subsequent injections of 5 mg/kg/week significantly decreased plasma cholesterol until day 6; plasma cholesterol returned to normal on day 10 (Fig. 4a). We then increased the dose to 7.5 mg/kg/week and observed a similar response; plasma cholesterol was reduced for 6 days and subsequently rebounded to normal levels (Fig. 4a). Increasing the dose to 10 mg/kg/week by injecting 5 mg/kg on 2 consecutive days reduced plasma cholesterol by $\sim 39\%$. Two subsequent 10 mg/kg/week injections reduced plasma cholesterol by 36–40% when compared with the PBS group. There were no significant differences in plasma triglycerides in these groups throughout the study. Mice were then subjected to euthanasia 6 days after the last injection. FPLC analysis of pooled plasma revealed reduced cholesterol levels in the VLDL/LDL fraction (Fig. 4b, left) with no effect on triglyceride (not shown). Quantification of areas under the curve revealed a 30% reduction of cholesterol in the VLDL/LDL fraction (Fig. 4b, right). The plasma of miR-30c mimic-injected mice had significantly lower apoB100 and apoB48, but apoA-I levels were not different (Fig. 4c). These long term studies involving multiple injections had no effect

MiR-30c Mimic and Hyperlipidemia

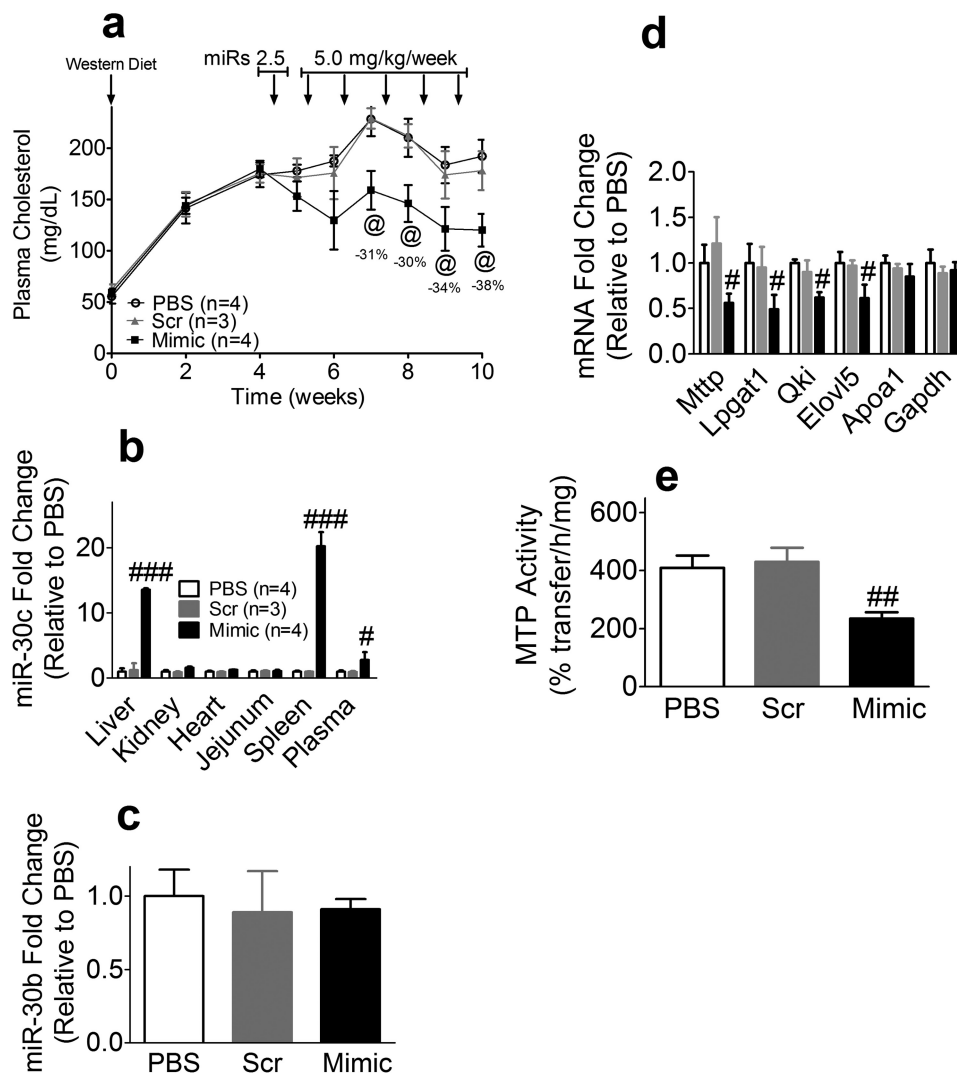


FIGURE 3. MiR-30c mimic causes regression of diet-induced hypercholesterolemia. Male C57BL/6J mice (8 weeks old) were fed a Western diet for 4 weeks and then injected weekly with PBS or increasing doses of Scr or miR-30c mimic for 6 weeks. Animals remained on Western diet during the entire experiment. *a*, plasma was collected from overnight fasted mice 6 days after every injection to measure cholesterol. *b*, 48 h after the last injection, tissues were collected to measure miR-30c levels. *c–e*, hepatic tissues were used to measure miR-30b levels (*c*), different indicated mRNAs (*d*), and MTP activity (*e*). The data are representative of two independent experiments. Statistical significance is represented as follows: #, $p < 0.05$; ##, $p < 0.01$; ###, $p < 0.001$ as determined by one-way analysis of variance (#) and Student *t* test (*p*) compared with the PBS group. Standard deviations are presented as error bars.

on plasma ALT, AST, and CK activities and phospholipids and food intake. Hepatic analysis of miR-30c levels revealed an ~4-fold increase in miR-30c levels. Furthermore, MTP mRNA was significantly reduced in the miR-30c mimic-injected group (Fig. 4*d*). Additionally, there was a 50% reduction in hepatic MTP, but not GAPDH, protein (Fig. 4*e*). In contrast, hepatic cholesterol, triglyceride, and phospholipids were not different between the treatment groups (not shown). These studies indicated that a single injection of miR-30c lowers plasma cholesterol in VLDL/LDL for about a week in a dose-dependent manner. Furthermore, multiple injections consistently reproduce these effects with no obvious long term adverse effects.

Mechanisms Explaining the Lowering of Plasma Cholesterol

MiR-30c Mimic Does Not Affect LDL Clearance—To understand physiological mechanisms for reductions in plasma cholesterol, we first aimed at studying whether miR-30c mimic

increases LDL clearance and therefore reduces plasma cholesterol. Male WT mice were fed a Western diet and injected with either PBS or miR-30c mimic for 2 weeks. MiR-30c mimic significantly reduced plasma cholesterol by –33% without affecting plasma triglyceride. LDL clearance studies showed that miR-30c mimic had no significant effect on apoB and apoA-I clearance (not shown), indicating that miR-30c mimic does not increase the rate of LDL clearance.

MiR-30c Mimic Reduces Hepatic, but Not Intestinal, Lipoprotein Production—To explain how miR-30c mimic reduces plasma cholesterol, we performed hepatic lipoprotein production studies in separate sets of animals (Fig. 5). MiR-30c mimic maximally reduced plasma cholesterol concentrations by 39% (not shown) as a result of changes in non-high density lipoproteins (Fig. 5*a*). However, it did not significantly affect triglycerides in the whole plasma or within different lipoprotein fractions (Fig. 5*b*). After the injection of poloxamer 407 to inhibit lipoprotein lipases (35), the miR-30c mimic group accumulated

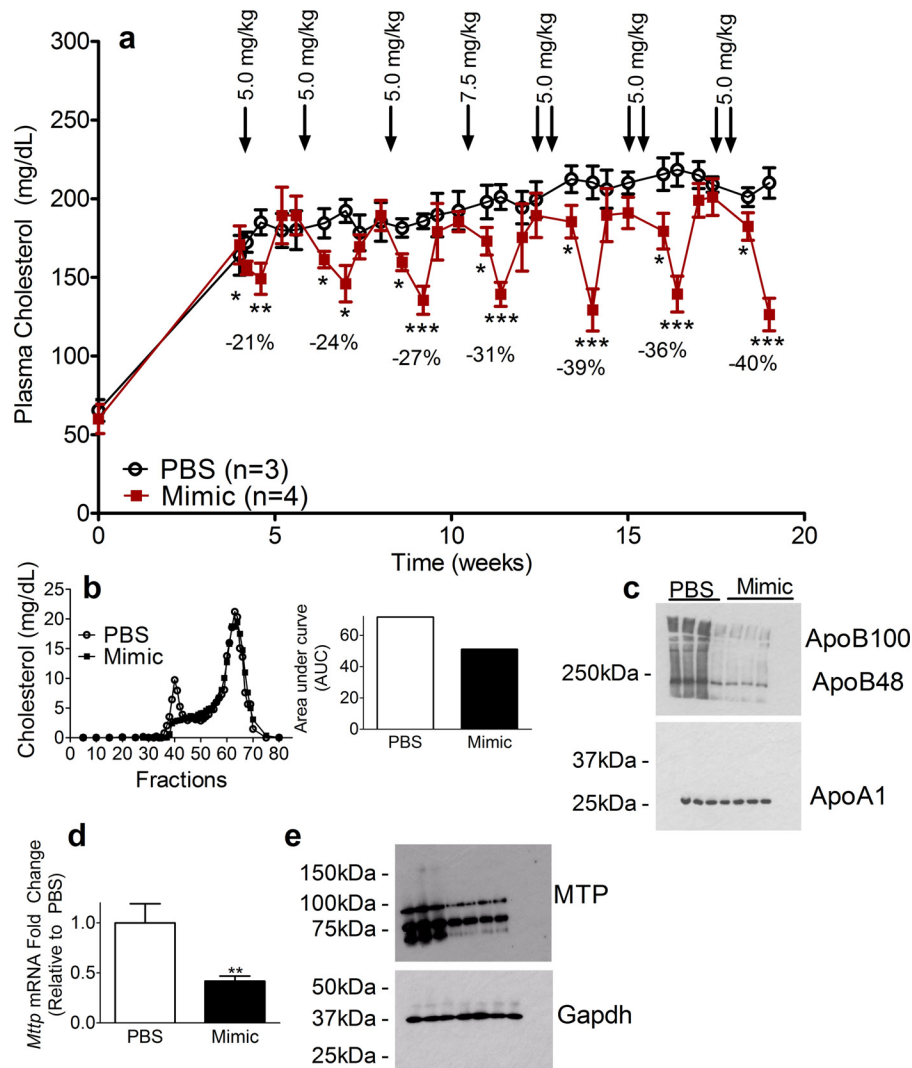


FIGURE 4. Time course and long term effects of escalating doses of miR-30c mimic. Female C57BL/6J mice (8 weeks old) were fed a Western diet for 4 weeks to induce hyperlipidemia and then injected with either PBS (control) or miR-30c mimic at different times as shown. Mice were fasted overnight before plasma was collected on days 2, 6, 10, and 14 after each injection. *a*, plasma was used to measure cholesterol. *b*, at the end, mice were euthanized, and plasma was collected 6 days after the last injection and subjected to FPLC to measure cholesterol (*left panel*) and the corresponding area under the curve in the VLDL and mimics groups (*right panel*) in the VLDL fraction. *c*, apoB and apoA-I were detected by Western blotting in individual mouse plasma sample. *d* and *e*, livers were collected to measure MTP mRNA (*d*) and protein (*e*). *, $p < 0.05$; **, $p < 0.01$; ***, $p < 0.001$. Standard deviations are presented as error bars.

lower amounts of plasma triglycerides (Fig. 5c) due to significantly reduced triglyceride production rates ($207 \text{ mg}\cdot\text{dl}^{-1}\cdot\text{h}^{-1}$) compared with controls ($334 \text{ mg}\cdot\text{dl}^{-1}\cdot\text{h}^{-1}$). Furthermore, the amounts of newly synthesized and secreted apoB100 and apoB48, but not apoA-I, were lower in the plasma of the miR-30c mimic group (Fig. 5d). These studies indicate that miR-30c mimic lowers hepatic production of triglyceride-rich apoB-containing lipoproteins.

Besides the liver, the intestine is another major organ involved in lipoprotein synthesis and secretion. Therefore, we asked whether miR-30c mimic also influences intestinal lipoprotein production. There were no significant differences in the absorption of lipids between the PBS and miR-30c mimic groups (Fig. 5, *e* and *f*). This is consistent with no accretions of miR-30c in the jejunum (Fig. 3e). Thus, intravenous injection of miR-30c mimic has no effect on intestinal lipid absorption as it is not delivered to the jejunum.

MiR-30c Mimic Does Not Lower Plasma Cholesterol in Liver-specific MTP-deficient Mice—To further test the hypothesis that miR-30c mimic reduces hepatic lipoprotein production primarily through suppression of MTP activity, we examined the effect of the mimic in Western diet-fed, liver-specific MTP-deficient (*Albumin-Cre:Mttp^{flax/flax}, L-Mttp^{-/-}*) mice that do not secrete lipoproteins from the liver (36). MiR-30c mimic had no effect on cholesterol and triglyceride in total plasma and different lipoprotein fractions (Fig. 6a and data not shown). Moreover, there were no significant differences in plasma ALT, AST, and CK activities between the PBS and mimic groups. Hepatic tissue analysis indicated that miR-30c levels were significantly increased (5-fold) in the mimic group, and predicted miR-30c targets were significantly lower in the mimic group compared with the PBS group, whereas those of non-target genes were not (Fig. 6b). More interestingly, as opposed to WT mice, miR-30c mimic significantly reduced hepatic cholesterol and triglyceride in *L-Mttp^{-/-}* (Fig. 6, *c*

MiR-30c Mimic and Hyperlipidemia

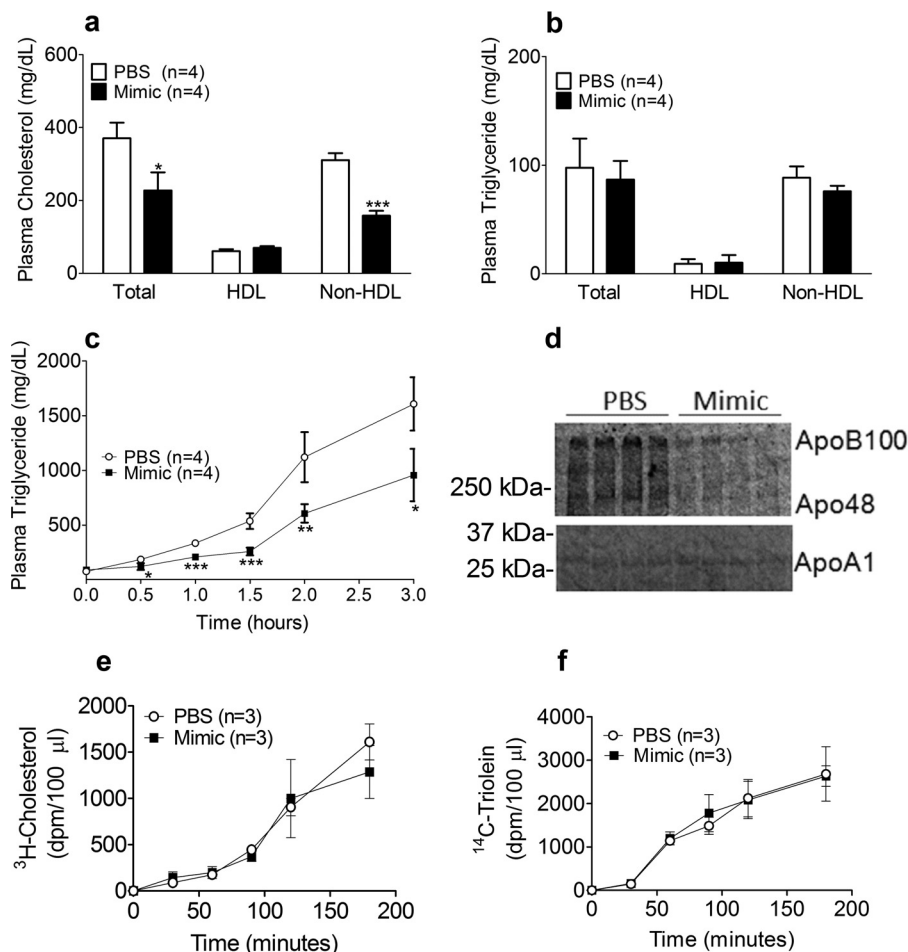


FIGURE 5. MiR-30c mimic reduces triglyceride-rich apoB-containing lipoprotein production. Male C57BL/6J mice ($n = 4$ per group) were fed a Western diet for 4 weeks and then weekly injected with PBS or miR-30c mimic (5.0 mg/kg) for 2 weeks. *a* and *b*, after overnight fasting, plasma was collected to measure cholesterol (*a*) and triglycerides (*b*) in different lipoprotein fractions after precipitation. *c* and *d*, 2 days after the last miR-30c or PBS injection, mice were fasted for 18 h and injected with poloxamer 407 and ³⁵S Pro-Mix to study hepatic lipoprotein production. *c*, a time course of changes in plasma triglyceride was measured. *d*, immunoprecipitation of apoB and apoA-1 in plasma obtained at 2 h. Values are shown relative to PBS. *, $p < 0.05$; **, $p < 0.01$; ***, $p < 0.001$ as determined by Student's *t* test. Standard deviations are presented as error bars. *e* and *f*, in a different set of animals, 2 days after the last injection of miR-30c or PBS, mice were injected with poloxamer 407 and gavaged with olive oil, cholesterol, [³H]cholesterol, and [¹⁴C]triolein. Time courses of cholesterol (*c*) and triglyceride (*d*) intestinal absorption were measured.

and *d*). These studies suggest that the effect of the mimic on plasma cholesterol is mainly through suppression of MTP. And, in the absence of MTP, miR-30c does not lower plasma cholesterol but does lower hepatic lipids.

Mechanisms Explaining the Absence of Hepatic Steatosis

MiR-30c Mimic Reduces Hepatic Lipid Synthesis Independently of MTP Function—To learn about the regulation of hepatic lipid metabolism by miR-30c and to understand how miR-30c mimic reduces hepatic lipoprotein production without increasing hepatic lipid concentrations, we performed hepatic fatty acid oxidation; *de novo* lipogenesis; and triglyceride, cholesterol, and phospholipid biosyntheses using fresh liver slices obtained from WT and *L-Mttp*^{-/-} mice in Figs. 2 and 6, respectively (Fig. 7). MiR-30c mimic did not affect fatty acid oxidation (Fig. 7*a*) but significantly reduced fatty acid, triglyceride, and cholesterol syntheses compared with PBS controls in WT mice (Fig. 7, *b–d*). Similarly, miR-30c treatment in *L-Mttp*^{-/-} mice did not affect fatty acid oxidation (Fig. 7*e*) but significantly reduced *de novo* lipogenesis as well as triglyceride

and cholesterol syntheses (Fig. 7, *f–h*). These studies suggest that miR-30c mimic reduces hepatic lipid synthesis independently of MTP, and this might avoid hepatic steatosis usually associated with reductions in lipoprotein production.

MiR-30c Mimic Prominently Suppresses Lipid Metabolic Pathways—To understand global effects of miR-30c on gene expression, we performed whole transcriptome analysis on the livers obtained from mice in Fig. 3. High throughput RNA-seq yielded an average of ~77 million reads per sample of which ~79% were mapped to the mouse transcriptome (supplemental Table S1).

MiR-30c mimic down-regulated 576 genes compared with both PBS and Scr (Fig. 8*a*). Surprisingly, a higher number of genes ($n = 1342$) were up-regulated by miR-30c mimic. Using miRHub, we observed that the down-regulated genes were significantly enriched for predicted target sites of miR-30c, but the up-regulated genes were not (Fig. 8*b*). Thus, the miR-30c mimic down-regulates a small set of genes expressed in the liver (~4%), many of which are likely direct miR-30c targets, and up-regulates a larger set of genes (~10%) via unknown indirect mechanisms.

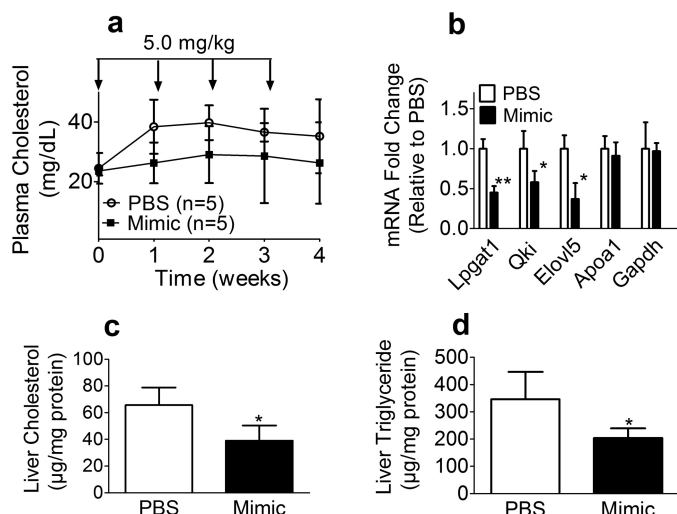


FIGURE 6. MiR-30c mimic does not reduce plasma cholesterol in liver-specific MTP deficient mice. Eight-week-old male *L-Mttp*^{-/-} mice were injected retro-orbitally with either PBS or miR-30c mimic (5.0 mg/kg) and started on a Western diet for 4 weeks. Mice were fasted overnight, and plasma was collected 4 days after each injection. *a*, cholesterol was measured in total plasma. *b–d*, livers were collected 48 h after the last injection to measure different mRNAs (*b*), cholesterol (*c*), and triglyceride (*d*). *, $p < 0.05$; **, $p < 0.01$ as determined by Student's *t* test. Standard deviations are presented as error bars.

Pathway enrichment analysis revealed that genes down-regulated by miR-30c mimic are over-represented in lipid metabolic processes (Fig. 8, *c* and *d*). Indeed, miR-30c mimic significantly reduced the expression of numerous genes encoding lipid synthesis enzymes such as *Lpin1*, *Lpin2*, *Gpam*, *Agpat6*, *Fads3*, *Fads2*, *Scd1*, *Elovl5*, and *Elovl6*, which might play an important role in diet-induced steatosis and obesity. These findings are consistent with reduced hepatic fatty acid and triglyceride syntheses observed in Fig. 7. Surprisingly, we observed significant increases in *Srebp-2* and *Pcsk9* levels. However, these increases were not accompanied with increases in cholesterol synthesis and LDL clearance.

Regression of Atherosclerosis by MiR-30c Mimic

The studies described above show that miR-30c reduces plasma cholesterol in hyperlipidemic mice by reducing hepatic lipoprotein production. To determine whether miR-30c mimic can cause regression of atherosclerosis, *ApoE*^{-/-} mice were fed a Western diet for 1 month, divided in two groups, and injected with either PBS or miR-30c mimic at a dose of 7.5 mg/kg/week for 4 weeks (Fig. 9). MiR-30c mimic significantly reduced plasma cholesterol up to 38% (Fig. 9*a*) without affecting plasma triglyceride, ALT, AST, and CK levels. Tissue analysis revealed significant increases in plasma, liver, and spleen miR-30c levels with no change in kidney, heart, and jejunum (Fig. 9*b*). Hepatic levels of putative miR-30c target genes (*Mttp*, *Lpgat1*, *QKI*, and *Elovl5*) were significantly reduced, whereas non-target genes (*ApoA1* and *Gapdh*) were not. MTP activity was significantly reduced in the mimic group (Fig. 9*c*). There were no differences in hepatic cholesterol and triglyceride levels. Furthermore, we visualized plaques at the aortic arches and detected fewer plaques in the mimic group compared with the PBS group (Fig. 9*d*). Oil Red O staining of aortas revealed ~30% less lipid staining in the miR-30c group (Fig. 9, *e* and *f*). These studies showed

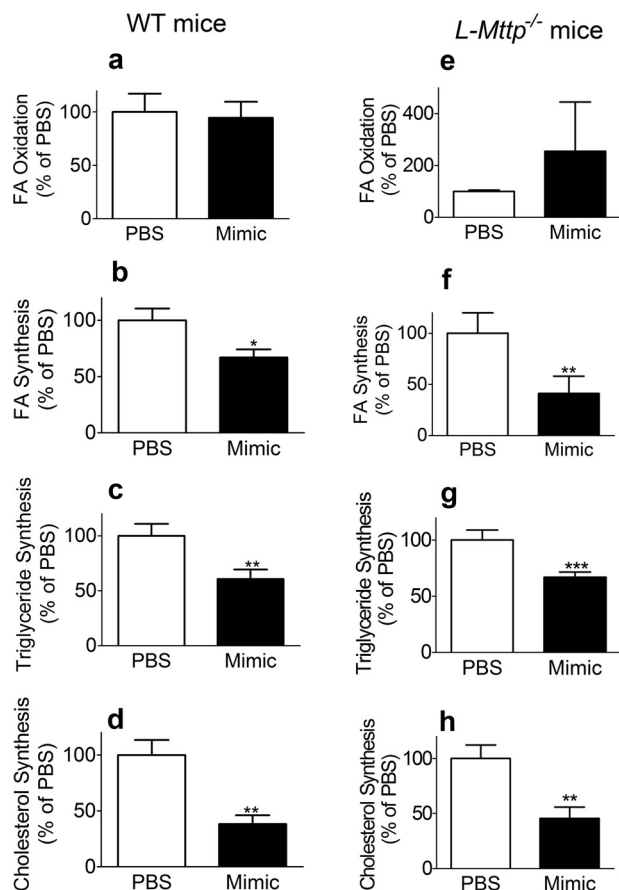


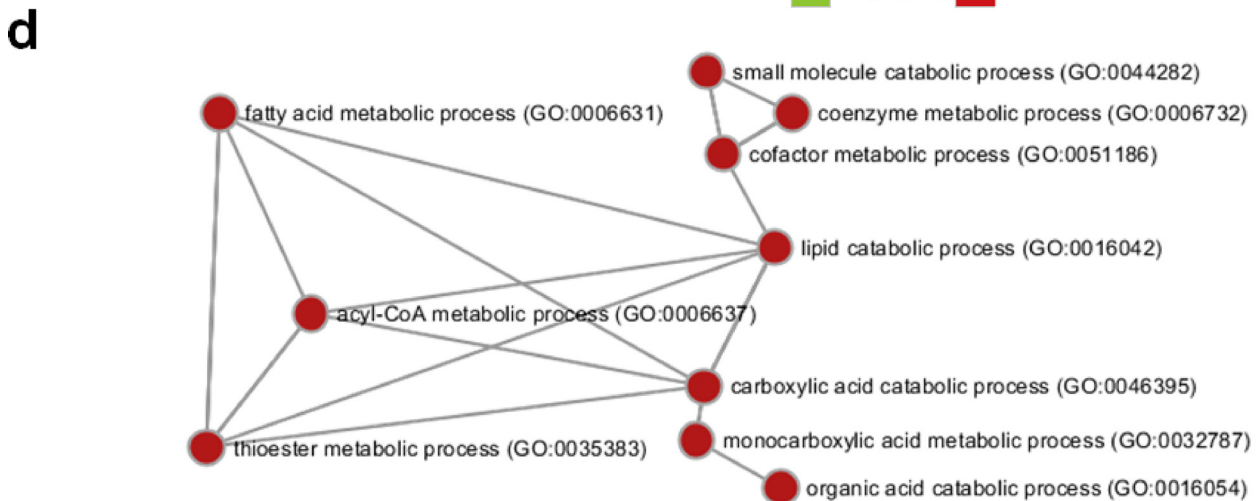
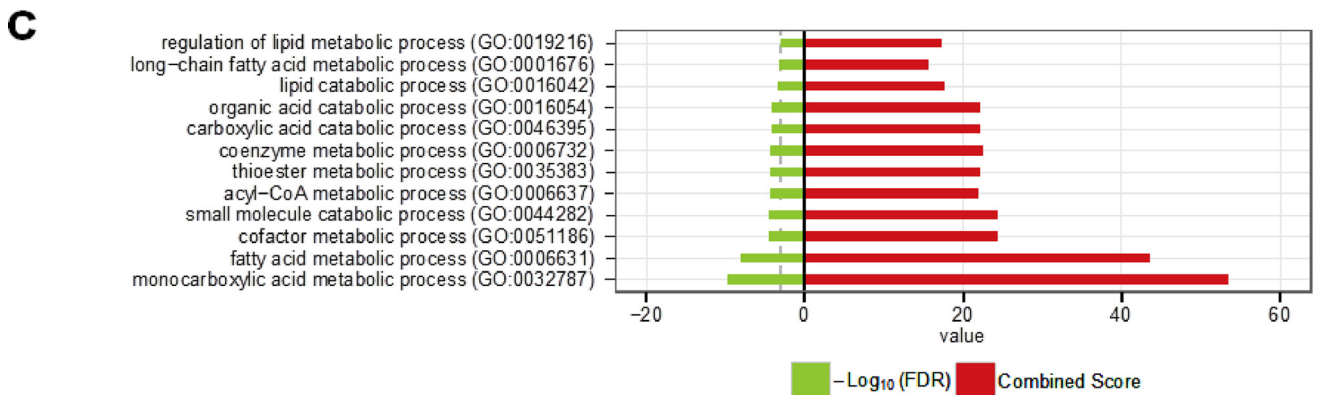
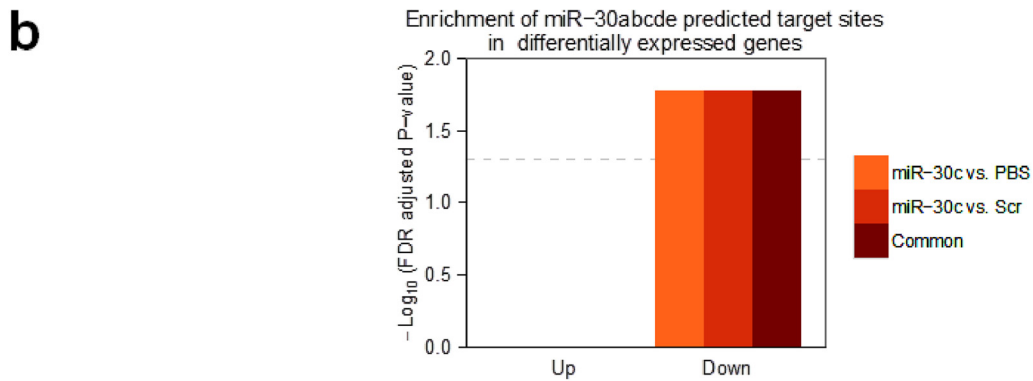
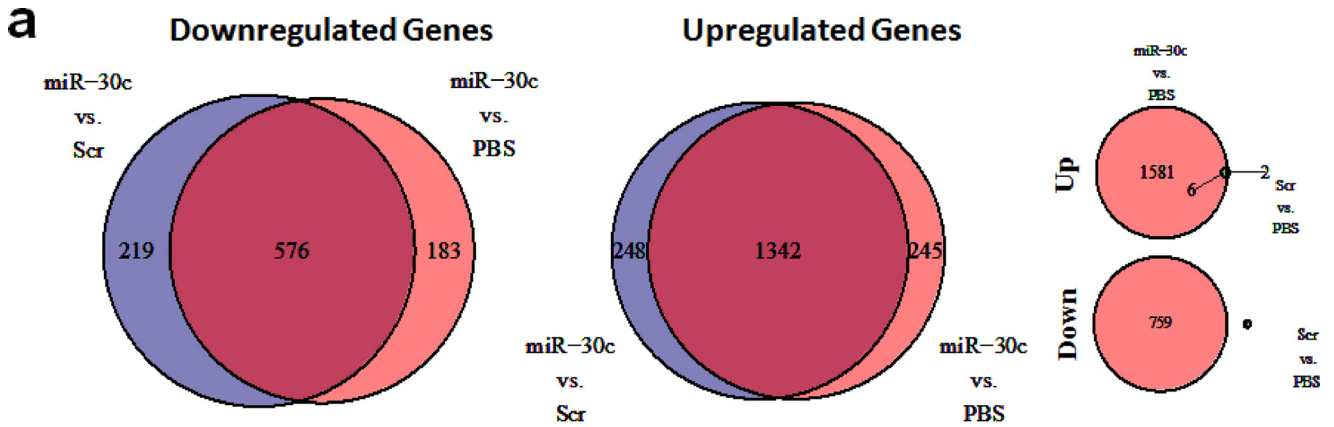
FIGURE 7. MiR-30c mimic reduces hepatic lipid synthesis independently of MTP function. *a–d*, WT liver slices from Fig. 2 were used to measure fatty acid (FA) oxidation (*a*) as well as fatty acid (*b*), triglyceride (*c*), and cholesterol (*d*) syntheses. *, $p < 0.05$; **, $p < 0.01$ as determined by Student's *t* test. *e–h*, liver slices from *L-Mttp*^{-/-} mice from Fig. 6 were used to measure fatty acid oxidation (*e*) as well as fatty acid (*f*), triglyceride (*g*), and cholesterol (*h*) syntheses. **, $p < 0.01$; ***, $p < 0.001$ as determined by Student's *t* test. Standard deviations are presented as error bars.

that the miR-30c mimic survives plasma excursions, reaches the liver, lowers plasma cholesterol, and causes regression of atherosclerosis without causing hepatosteatosis or increasing plasma transaminases.

Discussion

Previously, we showed that lentivirally mediated hepatic expression of miR-30c lowers plasma cholesterol and atherosclerosis in mice (34). Because lentiviral delivery of miR-30c would be formidable for therapeutic purposes, we evaluated the hypothesis that a synthetic miR-30c mimic might be a suitable treatment modality in both male and female mice. Here, we show for the first time that weekly injections of a miR-30c mimic elevate hepatic miR-30c levels with no significant effect on miR-30b expression. This treatment results in sustained reductions in plasma cholesterol levels in Western diet-fed male and female WT and *ApoE*^{-/-} mice, indicating equal efficiency in both genders. The effect of miR-30c was dose-dependent, and the maximum effect on plasma cholesterol was observed 6 days after each injection. Furthermore, we show that weekly injections of a miR-30c mimic also reduce atherosclerosis in Western diet-fed *ApoE*^{-/-} mice. These reductions in

MiR-30c Mimic and Hyperlipidemia



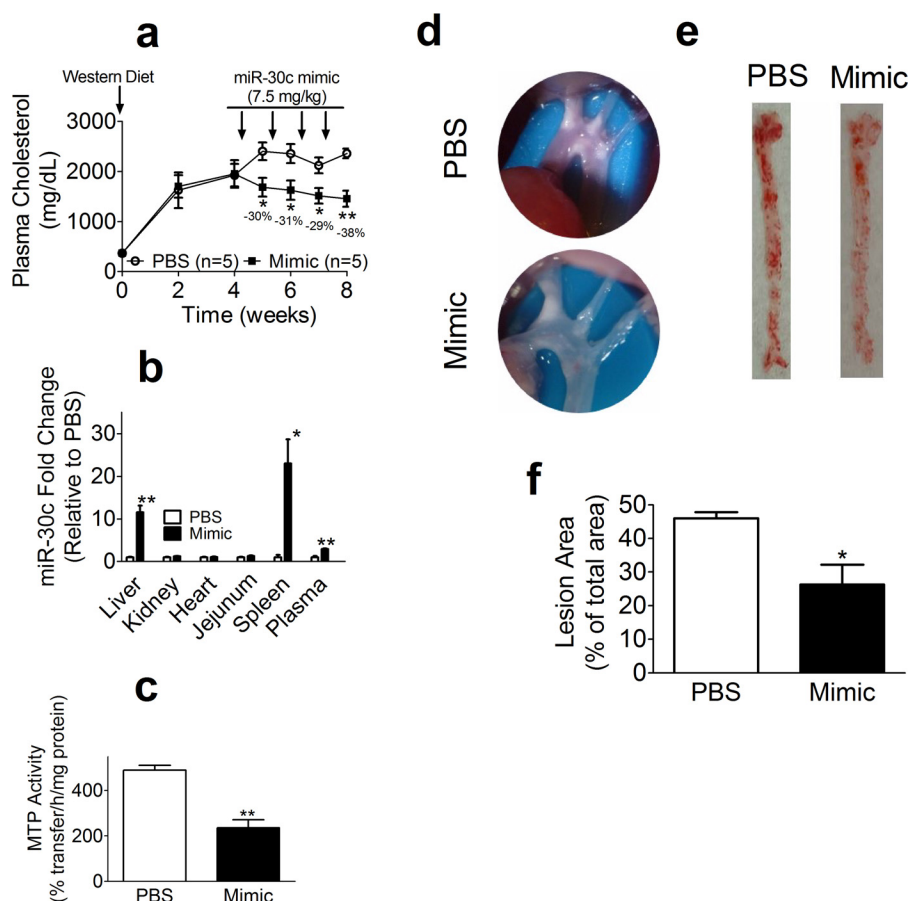


FIGURE 9. MiR-30c mimic causes regression of diet-induced atherosclerosis. Female *ApoE*^{-/-} mice (8 weeks old) were fed a Western diet for 4 weeks and then injected weekly with PBS or 7.5 mg/kg/week miR-30c mimic ($n = 5$ per group) for another 4 weeks. *a*, fasting plasma was collected 4 days after each injection to measure cholesterol. *b* and *c*, 48 h after the last injection, tissues were collected to measure miR-30c levels (*b*). Hepatic tissue was used to measure MTP activity (*c*). *d*, aortic arches were exposed and photographed. *e* and *f*, aortas were collected, fixed, stained with Oil Red O (*e*), and quantified (*f*). The data are representative of three experiments. *, $p < 0.05$; **, $p < 0.01$ as determined by Student's *t* test. Standard deviations are presented as error bars.

plasma cholesterol and atherosclerosis were not accompanied with increases in plasma ALT, AST, and CK, indicating that the miR-30c mimic was not causing any obvious liver and muscle injury. Thus, these studies suggest that miR-30c mimic could be developed into a safe, long lasting, and effective therapeutic agent for lowering plasma cholesterol.

MiR-30c mimic most likely reduces plasma cholesterol by lowering the production of apoB-containing lipoproteins through suppression of MTP activity as these reductions were not seen in *L-Mttp*^{-/-} mice. In contrast, miR-30c reduced hepatic fatty acid and triglyceride syntheses in *L-Mttp*^{-/-} mice, indicating that it affects these processes independently of MTP (34). Thus, the miR-30c mimic acts via MTP-dependent and

-independent mechanisms to control plasma and hepatic lipids, respectively.

MiR-30c mimic reduced lipoprotein production but did not cause steatosis usually associated with reductions in lipoprotein production. One possibility is that miR-30c modestly diminished MTP activity, making it insufficient to induce steatosis. Another possibility is that reductions in *de novo* lipogenesis and triglyceride synthesis mitigate steatosis associated with reductions in lipoprotein secretion. A clue for the balancing act between lipid synthesis and lipoprotein secretion came from studies in *L-Mttp*^{-/-} mice. In these mice, there were significant reductions in hepatosteatosis compared with controls, suggesting that, in the absence of lipoprotein secretion, reductions in

FIGURE 8. Global changes in hepatic gene expression pursuant to miR-30c mimic accretion. *a*, Venn diagrams showing the number of down-regulated (*left*) and up-regulated (*center*) genes shared between mimic versus PBS and mimic versus Scr, respectively. The numbers of up-regulated (*Up*) and down-regulated (*Down*) genes shared between mimic versus PBS and Scr versus PBS are shown. Genes that reached an expression threshold of counts per million > 1 in three or more samples were analyzed for differential expression. Genes were considered differentially expressed if they reached a ± 1.5 -fold change cutoff of ± 1.5 and false discovery rate (*FDR*) < 0.05 . *b*, miR-30abcde predicted target sites (these miRs share the same seed sequence) are enriched only in the genes significantly down-regulated by miR-30c mimic. Genes that reached an expression threshold of counts per million > 1 in three or more samples were analyzed for differential expression if they reached a ± 1.5 -fold change cutoff of ± 1.5 and *FDR* < 0.05 . The *y* axis shows the $-\log_{10}$ (*FDR*-adjusted *p* value) of the miR-30abcde miRHub enrichment score. *FDR* = 0.05 is indicated by the gray dashed line. "Common" represents differentially expressed genes common to both mimic versus PBS and mimic versus scrambled. *c* and *d*, gene ontology (*GO*) enrichment analysis of differentially expressed genes common to both mimic versus PBS and mimic versus Scr was conducted using Enrichr. *c*, all gene ontology biological process terms that reached an *FDR* cutoff of 0.001. *d*, a network of gene ontology biological process terms enriched in the down-regulated genes. Each *node* represents an enriched term, and each *link* indicates gene content overlap. Green bars show the \log_{10} (*FDR*), and red bars show the combined score, which is computed by multiplying the \log_{10} (*p* value) from a Fisher's exact test with the z-score of the deviation from the expected rank.

MiR-30c Mimic and Hyperlipidemia

de novo lipogenesis might lower hepatic lipids. Furthermore, comprehensive transcriptome analysis revealed that miR-30c mimic predominantly suppresses lipogenic programs in the liver. Consistent with this finding, physiological studies suggest that miR-30c mimic likely avoids hepatosteatosis in mice by reducing hepatic *de novo* lipogenesis and triglyceride synthesis. Thus, miR-30c might maintain hepatic lipids by inhibiting at least two pathways, lipid synthesis and lipoprotein secretion.

We did not see significant reductions in fasting plasma triglyceride. This was unexpected as miR-30c mimic reduced production of triglyceride-rich lipoproteins. No effect on plasma triglyceride is most likely secondary to complete hydrolysis of triglycerides by lipoprotein lipase in control mice. This can be tested in the future by studying the effect of miR-30c in lipoprotein lipase-deficient animals.

We used two controls, PBS and Scr, to evaluate the effects of miR-30c mimic. Remarkably, very few differences were found in the expression of genes and in the metabolic responses in PBS and Scr groups. In contrast, the mimic group showed significant differences compared with both controls. Thus, the response seen with miR-30c mimic is specific to its biological effect and is not related to RNA moiety or the vehicle used for its delivery.

RNA-seq analysis showed that miR-30c mimic down-regulated a small set (~4%) of genes expressed in the liver. These genes exhibited significant enrichment for miR-30c target sites. Surprisingly, it increased the expression of twice as many genes. There was no significant enrichment of miR-30c target sequence in the up-regulated genes, indicating that increases are not due to direct effects. Mechanisms involved in the up-regulation of genes need further investigation and may uncover novel regulatory mechanisms.

RNA-seq studies also revealed that miR-30c up-regulated SREBP-2 and PCSK9. Therefore, we had anticipated increased cholesterol synthesis and decreased lipoprotein clearance. However, biochemical and physiological studies showed that cholesterol synthesis was reduced and that LDL clearance was normal. It is unclear why there is no correlation between changes in mRNA levels of SREBP-2 and PCSK9 and expected physiologic output.

These studies clearly show that miR-30c mimic can lower plasma cholesterol and atherosclerosis. Although efficacious, this mimic therapy can be improved further. First, a better delivery method might avoid intravenous injections. Second, use of other lipid formulations or nanoparticles may reduce the amounts of mimic needed to lower plasma cholesterol. Third, the mimic can be modified further to increase resistance to ribonucleases. Fourth, modifications can be introduced to increase its affinity for argonaute proteins to improve target recognition. These and other improvements may increase the efficacy of miR-30c-based drugs so that smaller amounts can be administered with lesser frequency for long lasting plasma cholesterol reductions.

In short, we show that miR-30c mimics can be used to lower plasma cholesterol and atherosclerosis without causing steatosis and affecting plasma transaminases and creatine kinase activity. Mechanistic studies identify two pathways (Fig. 10) that are regulated by miR-30c that explain its beneficial thera-

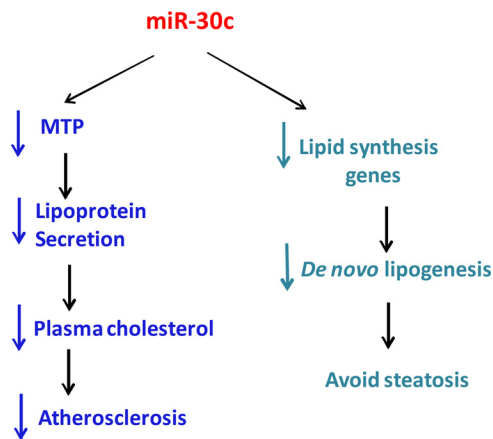


FIGURE 10. Regulation of atherosclerosis and hepatic steatosis by miR-30c. Our data show that miR-30c regulates expression of MTP and several genes involved in fatty acid synthesis to reduce lipoprotein production and lipid synthesis. Reduced plasma cholesterol may reduce atherosclerosis. Reduced hepatic lipid synthesis may avoid steatosis usually associated with diminished lipoprotein secretion.

peutic potential. First, it reduces MTP expression to lower hepatic lipoprotein production. Second, it suppresses hepatic lipid synthesis, and this might help avoid steatosis usually associated with reduction in lipoprotein production. These proof-of-concept and molecular studies provide strong impetus for more preclinical studies in other animal models such as non-human primates and subsequent human clinical trials.

Experimental Procedures

Materials— ^{14}C oleic acid, ^3H triolein, ^3H acetate, ^3H glycerol, and ^{35}S Pro-Mix were purchased from PerkinElmer Life Sciences. Chemicals and solvents were from Fisher Scientific.

Animals and Diet—Wild type and *ApoE*^{-/-} mice on a C57BL/6J background were bred at SUNY Downstate Medical Center. Mice were fed a Western diet containing 17, 48.5, 21.2, and 0.2% (by weight) protein, carbohydrates, fat, and cholesterol, respectively (TD 88137, Harlan Teklad). All animal experiments were approved by the Institutional Animal Use and Care Committee of SUNY Downstate Medical Center.

MiR-30c Mimic Delivery to Mice—We custom synthesized 1 g of highly purified mirVanaTM miRNA mimic (miR-30c) and a non-targeting Scr mimic (Life Technologies). For their *in vivo* delivery, Scr or miR-30c mimic was mixed with InvivoFectamine 2.0 (Life Technologies), incubated for 30 min at 50 °C, and dialyzed at room temperature for 90 min in 1 liter of diethyl pyrocarbonate-treated PBS, pH 7.4, with gentle agitation. This step is crucial to enhance encapsulation and remove destabilizing solvents. Dialyzed complexes were collected, and volumes were adjusted with PBS to obtain desired concentrations. Mice fed a Western diet were injected weekly with the indicated doses by retro-orbital injections. 48 h after the last injection, mice were euthanized, and tissues were harvested and stored at -80 °C for analysis.

Plasma and Tissue Lipid Measurements—Mice were fasted overnight (15 h) before blood was collected in EDTA-rinsed tubes from retro-orbital venous plexus. Blood was centrifuged at 8,000 rpm for 5 min, and plasma was collected to enzymati-

cally measure cholesterol and triglyceride concentrations using kits (Thermo Scientific). HDL lipids were measured after precipitating plasma apoB-containing lipoproteins by the addition of equal volumes of 0.4 M MgCl₂ and 9.7 mM phosphotungstic acid, pH 7.4. Lipids in apoB-containing lipoproteins were deduced by subtracting the concentrations of HDL lipids from total lipids. For hepatic lipid measurements, liver pieces (~50 mg) were homogenized in buffer K (1 mM Tris-Cl, 1 mM EGTA, and 1 mM MgCl₂, pH 7.6), and a portion was subjected to lipid extraction.

Plasma Enzymes—Plasma ALT, AST (Biotron Diagnostics), and CK (Fisher Scientific) were measured using kits according to the manufacturers' protocols.

Hepatic Triglyceride and ApoB Secretion—C57BL/6J mice were fasted for 18 h, injected intraperitoneally with poloxamer 407 (90 mg ml⁻¹; 500 μl) and ³⁵S Pro-Mix (0.3 μCi per mouse) intravenously. Blood was removed at the indicated time points. For apoB secretion, plasma (100 μl) was incubated with 1 μg of polyclonal antibody to apoB (Texas Academy Biosciences, Product ID 20A-G1) in NET buffer (50 mM Tris, pH 7.4, 150 mM NaCl, 5 mM EDTA, 0.5% Triton X-100, and 0.1% SDS) for 18 h. Protein A/G-agarose beads (Santa Cruz Biotechnology) were added to pull down apoB. Immunoprecipitated proteins were separated by 5% SDS-PAGE (apoB) or 12% SDS-PAGE (apoA-I) and exposed to PhosphorImager screens. Bands were visualized with a Storm 860 device (Amersham Biosciences) and quantified by ImageJ.

In Vivo Absorption of Lipids—C57BL/6J mice were injected intraperitoneally with poloxamer 407 (90 mg ml⁻¹; 500 μl). After 1 h, mice were fed a mixture of 2 μCi of [¹⁴C]cholesterol, 1 μCi [³H]triolein, and 2 g/liter cholesterol (Sigma) in 50 μl of olive oil. Blood was collected retro-orbitally at the indicated time points, and plasma was used for liquid scintillation counting.

ApoB Secretion from Cells—Huh-7 cells (250,000 cells/well in a 6-well plate) were maintained in Dulbecco's modified Eagle's medium (DMEM) containing 10% fetal bovine serum (FBS), 1% penicillin-streptomycin, and 1% L-glutamine in T75 flasks at 37 °C and 5% CO₂ and transfected with either Scr or miR-30c mimic using RNAiMAX (Invitrogen) according to the manufacturer's instructions. The next day, 1 ml of fresh DMEM containing 10% FBS was added, cells were collected after 10 h, protease inhibitor mixture (Roche Applied Science) was added, cells were centrifuged, and the supernatant was used to measure apoB by ELISA (37).

MTP Activity Determination—Huh-7 cells or tissues (~50 mg) were supplemented with a protease inhibitor mixture at 1 mg/ml. Then samples were homogenized in 1 ml of buffer K and centrifuged (13,000 rpm, 30 min, 4 °C), and supernatants were used for protein quantification and MTP assay using a fluorescently labeled triglyceride transfer kit (Chylos, Inc.) (38).

mRNA Quantifications by Quantitative RT-PCR—Blood was collected in EDTA-rinsed capillaries (Fisherbrand). Plasma (200 μl) was mixed with an equal volume of RNAGents Denaturing Solution (Promega) and incubated for 5 min at room temperature. Next, 25 fmol of synthetic microRNA-39* from *Caenorhabditis elegans* (cel-miR-39*, Life Technologies, 4464066) were added as a spiked-in control. Then 1 ml of TRIzol was added to the mixture, mixed vigorously for 10 s, and

TABLE 1
Quantitative RT-PCR primers and miR sequences

Gene	Forward Primer	Reverse Primer
Mouse ApoB	tccatattccagacaacctctc	gtttatfttggctctgtcattggt
Mouse ApoA1	Ggccgtggetctgtgttt	ggttcattctgctgccatac
Mouse MTP	Gaccacctggatccata	agcctggtgaaaggcttat
Mouse ELOVL5	Gtctccatcccgccat	tgatttcagcaaacactgga
Mouse LPGAT1	tttagcaccgaggaaaat	ggcctctgattgcattct
Mouse ACOX1	aagaftcattctcaacagccc	ctggacagactctgagctgc
Mouse NCOR1	agaactctgatgtttctccag	ctggagacttgctggtata
Mouse OXI	ctggacgagaaattagcagat	actgccatttaactgctcattg
18s rRNA	Agtcctgcccctttgacaca	gatccgaggtcactaac

miR Sequences	
Scr	ucacaaccuccuagaagaaguaga
miR-30c mimic	uguaaacaucuccuacucucagc

incubated for 10 min at room temperature. After adding 200 μl of chloroform, the mixture was mixed on a vortex for 30 s and allowed to stand for 5 min at room temperature. Following centrifugation (12,000 rpm, 15 min, 4 °C), the aqueous phase was transferred to a new tube, and glycogen (Thermo Scientific) was added at 1 μg/μl per sample. Subsequently, samples were mixed with isopropanol and incubated at -80 °C for 2 h. Glycogen enhances RNA recovery during alcohol precipitation. Samples were centrifuged (10,000 rpm, 15 min, 4 °C), supernatants were discarded, and pellets were rinsed with cold 70% ethanol, air-dried for 10 min, and dissolved in diethyl pyrocarbonate-treated water.

For gene expression, first strand cDNA was synthesized with the Omniscript RT kit (Qiagen) and used for quantitative RT-PCR (qPCR Core kit for SYBR Green I, Eurogentec), and the C_t values for each mRNA were normalized to 18S. For miR quantification, cDNA was synthesized with the TaqMan MicroRNA Reverse Transcription kit (Applied Biosystems, 4366597) and used for quantitative RT-PCR. MiR analysis in cells and tissues was performed using the ΔΔC_t method with normalization to small nucleolar RNA 202 or U6 and is presented as arbitrary units. For miR-30c analysis in plasma, cel-miR-39* levels were measured using their specific TaqMan microRNA assays (Life Technologies, 464312) and used for the normalization of miR-30c levels. Primers used for mRNA quantification were designed using PrimerExpress 3.0 (Applied Biosystems) and are listed in Table 1. Primers specific for miR-30c, small nucleolar RNA 202, and U6 were purchased from Life Technologies.

Western Blotting Analyses—Liver tissues (50 mg) were homogenized in buffer K (1 ml) containing protease inhibitor mixture. Proteins (~20 μg) were resolved by SDS-PAGE (8%). A monoclonal mouse antibody to mouse MTP (BD Biosciences, 612022) and a rabbit antibody to mouse GAPDH (Santa Cruz Biotechnology, sc-20356) were diluted 1:1000 and used as the primary antibodies. Mouse Alexa Fluor 633 (Life Technologies, A21052 and A21082, respectively) were used, and blots were visualized using a Storm 860 device.

Fatty Acid Oxidation, de Novo Lipogenesis, and Triglyceride Synthesis—For fatty acid oxidation, fresh liver slices were incubated with [¹⁴C]oleic acid (0.3 μCi) for 2 h, and radiolabeled CO₂ was trapped with a filter paper soaked with phenylethylamine. For *de novo* lipogenesis, fresh liver slices were incubated with [³H]acetate (0.2 μCi), and lipids were extracted after saponification (36). Triglyceride synthesis was studied by incubating liver slices with [³H]glycerol (0.5 μCi), extracting lipids,

MiR-30c Mimic and Hyperlipidemia

and separating them on a silica 60 thin layer chromatography plate using a solvent mixture of diethyl ether, benzene, ethanol, and acetic acid at a ratio of 50:40:2:0.2. Counts were measured in a scintillation counter (Beckman LS 6000 TA).

Aortic Plaque Analyses—The aortic arches were dissected and exposed for photography. Lipids in fatty streaks were visualized on the aorta with Oil Red O staining and quantified with ImageJ (39, 40).

RNA Sequencing—RNA was isolated using a Norgen Animal Tissue Purification kit (Norgen). Briefly, 15 mg of flash frozen liver tissue was homogenized in lysis buffer using a 1.4-mm ceramic lysing matrix (MP Biomedicals). RNA was purified according to the manufacturer's instructions, including the optional on-column DNase I treatment. RNA was quantified using Nanodrop 2000, and RNA quality was assessed using an Agilent RNA 6000 Nano kit and Agilent 2100 Bioanalyzer. TruSeq stranded mRNA libraries were prepared and paired-end sequenced on a HiSeq 2500 sequencer with three to four samples per lane at the University of North Carolina High Throughput Sequencing Facility. Samples were demultiplexed using CASAVA/bcl2fastq (v1.8.4). Data qualities were assessed using Fastqc (v0.11.3) and aligned to the UCSC mm10 reference genome and BOWTIE index using Mapslice (v2.1.4). The “-fusion” parameter was used to search for both canonical and semicanonical splice junctions. Alignments were sorted using samtools (v0.1.19) and bedtools (v2.17.0). Multicov was used to generate isoform count tables for differential gene expression analysis using the UCSC mm10 known gene reference table, which was accessed on June 9, 2015 and converted to bed format. Isoform counts were read into R version 3.1.2 (October 31, 2014). By taking the maximum count of all isoforms for a given gene, we generated a table of gene counts. Genes were filtered for low expression using the criterion counts per million >1 in three or more samples, and edgeR/3.8.6 was then used to normalize remaining counts and conduct differential gene expression analysis. RNA-seq data have been submitted to the Gene Expression Omnibus (GEO) under accession number GSE70352.

Statistics—Data are presented as the mean \pm S.D. ($p < 0.05$). The statistical significance was determined by Student's *t* test or one-way or two-way analysis of variance (GraphPad Prism), and significant differences $p < 0.05$, $p < 0.01$, and $p < 0.001$ are symbolized as *, #, or @, respectively.

Author Contributions—S. I. designed and performed experiments, analyzed data, and wrote a draft of the paper. X. P. performed lipid syntheses, fatty acid oxidation, VLDL production, and intestinal absorption experiments. J. I. taught S. I. animal studies, MTP activity measurement, lipid measurement, lipoprotein precipitation, and atherosclerosis techniques and participated in radiolabeling and FPLC experiments. B. C. E. P. performed RNA-seq studies, analyzed data, and plotted the corresponding figures. P. S. supervised the RNA-seq studies and revised the manuscript. M. M. H. conceived the ideas, designed and discussed experiments, supervised the progress, and thoroughly edited the manuscript.

References

1. Go, A. S., Mozaffarian, D., Roger, V. L., Benjamin, E. J., Berry, J. D., Borden, W. B., Bravata, D. M., Dai, S., Ford, E. S., Fox, C. S., Franco, S., Fullerton, H. J., Gillespie, C., Hailpern, S. M., and Heit, J. A. (2013) Heart disease and stroke statistics—2013 update: a report from the American Heart Association. *Circulation* **127**, e6–e245
2. Goff, D. C., Jr., Lloyd-Jones, D. M., Bennett, G., Coady, S., D'Agostino, R. B., Gibbons, R., Greenland, P., Lackland, D. T., Levy, D., O'Donnell, C. J., Robinson, J. G., Schwartz, J. S., Shero, S. T., Smith, S. C., Jr., and Sorlie, P. (2014) 2013 ACC/AHA guideline on the treatment of blood cholesterol to reduce atherosclerotic cardiovascular risk in adults: a report of the American College of Cardiology/American Heart Association Task Force on Practice Guidelines. *Circulation* **129**, Suppl. 2, S49–S73
3. Robinson, J. G., and Gidding, S. S. (2014) Curing atherosclerosis should be the next major cardiovascular prevention goal. *J. Am. Coll. Cardiol.* **63**, 2779–2785
4. Grundy, S. M., Cleeman, J. I., Merz, C. N., Brewer, H. B., Jr., Clark, L. T., Hunninghake, D. B., Pasternak, R. C., Smith, S. C., Jr., Stone, N. J., National Heart, Lung, and Blood Institute, American College of Cardiology Foundation, and American Heart Association (2004) Implications of recent clinical trials for the National Cholesterol Education Program Adult Treatment Panel III guidelines. *Circulation* **110**, 227–239
5. LaRosa, J. C., Grundy, S. M., Waters, D. D., Shear, C., Barter, P., Fruchart, J. C., Gotto, A. M., Greten, H., Kastelein, J. J., Shepherd, J., Wenger, N. K., and Treating to New Targets (TNT) Investigators (2005) Intensive lipid lowering with atorvastatin in patients with stable coronary disease. *N. Engl. J. Med.* **352**, 1425–1435
6. Blumenthal, R. S. (2000) Statins: effective antiatherosclerotic therapy. *Am. Heart J.* **139**, 577–583
7. Ehrenstein, M. R., Jury, E. C., and Mauri, C. (2005) Statins for atherosclerosis—as good as it gets? *N. Engl. J. Med.* **352**, 73–75
8. Rader, D. J., and Kastelein, J. J. (2014) Lomitapide and mipomersen: two first-in-class drugs for reducing low-density lipoprotein cholesterol in patients with homozygous familial hypercholesterolemia. *Circulation* **129**, 1022–1032
9. Stoekenbroek, R. M., Kastelein, J. J., and Huijgen, R. (2015) PCSK9 inhibition: the way forward in the treatment of dyslipidemia. *BMC Med.* **13**, 258
10. Stroes, E., Colquhoun, D., Sullivan, D., Civeira, F., Rosenson, R. S., Watters, G. F., Bruckert, E., Cho, L., Dent, R., Knusel, B., Xue, A., Scott, R., Wasserman, S. M., Rocco, M., and GAUSS-2 Investigators (2014) Anti-PCSK9 antibody effectively lowers cholesterol in patients with statin intolerance: the GAUSS-2 randomized, placebo-controlled phase 3 clinical trial of evolocumab. *J. Am. Coll. Cardiol.* **63**, 2541–2548
11. Raal, F. J., Stein, E. A., Dufour, R., Turner, T., Civeira, F., Burgess, L., Langslet, G., Scott, R., Olsson, A. G., Sullivan, D., Hovingh, G. K., Cariou, B., Gouni-Berthold, I., Somaratne, R., and Bridges, I. (2015) PCSK9 inhibition with evolocumab (AMG 145) in heterozygous familial hypercholesterolemia (RUTHERFORD-2): a randomised, double-blind, placebo-controlled trial. *Lancet* **385**, 331–340
12. Robinson, J. G., Farnier, M., Krempf, M., Bergeron, J., Luc, G., Averna, M., Stroes, E. S., Langslet, G., Raal, F. J., El Shahawy, M., Koren, M. J., Lepor, N. E., Lorenzato, C., Pordy, R., and Chaudhari, U. (2015) Efficacy and safety of alirocumab in reducing lipids and cardiovascular events. *N. Engl. J. Med.* **372**, 1489–1499
13. Finkel, J. B., and Duffy, D. (2015) 2013 ACC/AHA cholesterol treatment guideline: paradigm shifts in managing atherosclerotic cardiovascular disease risk. *Trends Cardiovasc. Med.* **25**, 340–347
14. Cornier, M. A., and Eckel, R. H. (2015) Non-traditional dosing of statins in statin-intolerant patients—is it worth a try? *Curr. Atheroscler. Rep.* **17**, 475
15. Lipinski, M. J., Benedetto, U., Escarcega, R. O., Biondi-Zoccai, G., Lhermusier, T., Baker, N. C., Torguson, R., Brewer, H. B., Jr., and Waksman, R. (2016) The impact of proprotein convertase subtilisin-kexin type 9 serine protease inhibitors on lipid levels and outcomes in patients with primary hypercholesterolemia: a network meta-analysis. *Eur. Heart J.* **37**, 536–545
16. Hussain, M. M., Shi, J., and Dreizen, P. (2003) Microsomal triglyceride transfer protein and its role in apolipoprotein B-lipoprotein assembly. *J. Lipid Res.* **44**, 22–32
17. Hussain, M. M., Rava, P., Walsh, M., Rana, M., and Iqbal, J. (2012) Multiple functions of microsomal triglyceride transfer protein. *Nutr. Metab.* **9**, 14
18. Zimmermann, T. S., Lee, A. C., Akinc, A., Bramlage, B., Bumcrot, D.,

- Fedoruk, M. N., Harborth, J., Heyes, J. A., Jeffs, L. B., John, M., Judge, A. D., Lam, K., McClintock, K., Nechev, L. V., and Palmer, L. R. (2006) RNAi-mediated gene silencing in non-human primates. *Nature* **441**, 111–114
19. Ricotta, D. N., and Frishman, W. (2012) Mipomersen: a safe and effective antisense therapy adjunct to statins in patients with hypercholesterolemia. *Cardiol. Rev.* **20**, 90–95
 20. Samaha, F. F., McKenney, J., Bloedon, L. T., Sasiela, W. J., and Rader, D. J. (2008) Inhibition of microsomal triglyceride transfer protein alone or with ezetimibe in patients with moderate hypercholesterolemia. *Nat. Clin. Pract. Cardiovasc. Med.* **5**, 497–505
 21. Cuchel, M., Meagher, E. A., du Toit Theron, H., Blom, D. J., Marais, A. D., Hegele, R. A., Averna, M. R., Sirtori, C. R., Shah, P. K., Gaudet, D., Stefanutti, C., Vigna, G. B., Du Plessis, A. M., Propert, K. J., and Sasiela, W. J. (2013) Efficacy and safety of a microsomal triglyceride transfer protein inhibitor in patients with homozygous familial hypercholesterolaemia: a single-arm, open-label, phase 3 study. *Lancet* **381**, 40–46
 22. Cuchel, M., Bloedon, L. T., Szapary, P. O., Kolansky, D. M., Wolfe, M. L., Sarkis, A., Millar, J. S., Ikewaki, K., Siegelman, E. S., Gregg, R. E., and Rader, D. J. (2007) Inhibition of microsomal triglyceride transfer protein in familial hypercholesterolemia. *N. Engl. J. Med.* **356**, 148–156
 23. Hussain, M. M., and Bakillah, A. (2008) New approaches to target microsomal triglyceride transfer protein. *Curr. Opin. Lipidol.* **19**, 572–578
 24. Rizzo, M., and Wierzbicki, A. S. (2011) New lipid modulating drugs: the role of microsomal transport protein inhibitors. *Curr. Pharm. Des.* **17**, 943–949
 25. Cuchel, M., and Rader, D. J. (2013) Microsomal transfer protein inhibition in humans. *Curr. Opin. Lipidol.* **24**, 246–250
 26. Fernández-Hernando, C., Suárez, Y., Rayner, K. J., and Moore, K. J. (2011) MicroRNAs in lipid metabolism. *Curr. Opin. Lipidol.* **22**, 86–92
 27. Irani, S., and Hussain, M. M. (2015) Role of microRNA-30c in lipid metabolism, adipogenesis, cardiac remodeling and cancer. *Curr. Opin. Lipidol.* **26**, 139–146
 28. Bartel, D. P. (2004) MicroRNAs: genomics, biogenesis, mechanism, and function. *Cell* **116**, 281–297
 29. Bartel, D. P. (2009) MicroRNAs: target recognition and regulatory functions. *Cell* **136**, 215–233
 30. Izaurre, E. (2015) Gene regulation. Breakers and blockers—miRNAs at work. *Science* **349**, 380–382
 31. van Rooij, E., and Kauppinen, S. (2014) Development of microRNA therapeutics is coming of age. *EMBO Mol. Med.* **6**, 851–864
 32. Qiu, Z., and Dai, Y. (2014) Roadmap of miR-122-related clinical application from bench to bedside. *Expert Opin. Investig. Drugs* **23**, 347–355
 33. Bouchie, A. (2013) First microRNA mimic enters clinic. *Nat. Biotechnol.* **31**, 577
 34. Soh, J., Iqbal, J., Queiroz, J., Fernandez-Hernando, C., and Hussain, M. M. (2013) MicroRNA-30c reduces hyperlipidemia and atherosclerosis by decreasing lipid synthesis and lipoprotein secretion. *Nat. Med.* **19**, 892–900
 35. Millar, J. S., Cromley, D. A., McCoy, M. G., Rader, D. J., and Billheimer, J. T. (2005) Determining hepatic triglyceride production in mice: comparison of poloxamer 407 with Triton WR-1339. *J. Lipid Res.* **46**, 2023–2028
 36. Khatun, I., Zeissig, S., Iqbal, J., Wang, M., Curiel, D., Shelness, G. S., Blumberg, R. S., and Hussain, M. M. (2012) Phospholipid transfer activity of MTP promotes assembly of phospholipid-rich apoB-containing lipoproteins and reduces plasma as well as hepatic lipids in mice. *Hepatology* **55**, 1356–1368
 37. Bakillah, A., Zhou, Z., Luchoomun, J., and Hussain, M. M. (1997) Measurement of apolipoprotein B in various cell lines: correlation between intracellular levels and rates of secretion. *Lipids* **32**, 1113–1118
 38. Athar, H., Iqbal, J., Jiang, X. C., and Hussain, M. M. (2004) A simple, rapid, and sensitive fluorescence assay for microsomal triglyceride transfer protein. *J. Lipid Res.* **45**, 764–772
 39. Iqbal, J., Queiroz, J., Li, Y., Jiang, X. C., Ron, D., and Hussain, M. M. (2012) Increased intestinal lipid absorption caused by *Ire1 β* deficiency contributes to hyperlipidemia and atherosclerosis in apolipoprotein E-deficient mice. *Circ. Res.* **110**, 1575–1584
 40. Pan, X., Jiang, X. C., and Hussain, M. M. (2013) Impaired cholesterol metabolism and enhanced atherosclerosis in clock mutant mice. *Circulation* **128**, 1758–1769